8. Yu. A. Buevich and Yu. A. Korneev, "On heat and mass transfer in a disperse medium," Zh. Prikl. Mekh. Tekh. Fiz., No. 4, 79-87 (1974).
9. D. A. Frank-Kamanetskii, Diffusion and Heat Transfer in Chemical Kinetics, Plenum Publ. (1969).

HEAT TRANSFER AND CRYODEPOSIT PROPERTIES IN SOLID-STATE CONDENSATION

V. B. Lisovskii

UDC 536.423.4

An expression is derived for the effective thermal conductivity, which agrees with experiment. A study is made of heat transfer in solid-state condensation, and working formulas are derived.

Solid-state condensation or desublimation has not been extensively discussed in the literature, in contrast say to boiling. Solid-state condensation is used in some processes in chemical engineering and in cryogenic pumps. If the temperature of the cold surface is below the triple point, the vapor condenses directly to the solid state. It is familiar that water vapor will deposit as frost from air on cold surfaces. In all cases, the deposit adversely affects the heat transfer as it insulates the surface, and the removal requires the process or pump to be shut down.

The growth of the solid phase is a complicated nonstationary process involving various heat- and mass-transfer mechanisms. It can be represented as a boundary-value problem with a mobile boundary, which is characterized by heat and mass transfer through the growing layer of solid phase. The processes within the layer are such that the boundary layer can be considered as quasistationary.

The layer of solid phase is a porous body. In accordance with the conditions of formation, it has low density and high porosity, or conversely high density and low porosity. The temperature gradient in the layer produces vapor migration in condensation. Therefore, the density and thermal conductivity alter during the condensation.

Solid-state condensation on cold surfaces has been examined with an apparatus containing a vacuum chamber, in which a thermally insulated vessel containing liquid nitrogen was placed, which had an open condensation surface of diameter 56 mm. Condensable vapors were admitted (freon 13 and acetone) through a system including an RS-3A rotameter, damping capillary, fine-adjustment leak, and nozzle with porous baffle providing a vapor flow uniform over the cross section. The heat flux was determined from the loss of liquid nitrogen by boiling. The temperature of the cold surface was monitored by four copper–constantan thermocouples and recorded by an F-30 digital voltmeter. The pressure was measured with an oil gauge read by means of a cathetometer, which provided a sensitivity of 0.01 mm in the range 0.1-1.5 mm Hg. The surface temperature and the layer thickness were determined with a mobile probe fitted with a micrometer screw giving a displacement accuracy of 0.01 mm. The maximum layer thickness was 5 mm.

The deposit was observed and photographed with an illumination system. As there are no standard data, we determined the following parameters of the monolithic solid in separate experiments: heat sublimation, density, and thermal conductivity.

The formation of the solid phase begins with the production of thin needles growing from the cold surface. Then the tops of the needles, which had attained a length of 2-3 mm, began to produce whiskers, which were interwoven. The structure became more complicated. The growth of the solid continued on the outside. There were considerable effects on the structure

A. V. Lykov Institute of Heat and Mass Transfer, Academy of Sciences of the Belorussian SSR, Minsk. Translated from Inzhenerno-Fizicheskii Zhurnal, Vol. 50, No. 2, pp. 278-285, February, 1986. Original article submitted December 7, 1984.

0022-0841/86/5002-0207$12.50

from the vapor pressure and the supercooling of the cold surface relative to the triple point. At high partial pressures $P_v/P > 0.5$ and high supercooling, the material had low density and high porosity, while at low partial pressure and with small supercooling (less than 10°C), it had high density and low porosity.

The quasistationary condition is important to the analysis, because isothermal conditions applied at the cold surface, while the surface temperature of the deposit increased slowly. The thermal-conductivity measurement was based on the energy equation

$$\frac{d}{dt}\left(k_{\text{eff}}\frac{dT}{dx}\right) = -r_c\frac{dm}{dx}. \tag{1}$$

The right side incorporates the contribution from the phase transition on condensation within the porous solid. This expression may be written as $\frac{d}{dx}\left(k_v\frac{dT}{dx}\right)$, where k_V is the contribution to the thermal conductivity from the phase transition. On integration we get $K\frac{dT}{dx} = q_0$, where q_0 is the constant heat flux through the cold wall. This expression is used in determining the thermal conductivity. We also assumed that the temperature distribution in the solid was linear, which is close to realistic, which gives $dT/dx = (T_S - T_W)/\delta$.

These structures are similar to those that have been described for water frost, so we use the models of [1, 2] to calculate the thermal conductivity (for water vapor deposits) and extend them to deposits of other substances.

Two types of structure have been mentioned, which can be represented as in Fig. 1 in the form of sets of cylinders of the solid produced by vapor diffusion together with spheres having much lower thermal conductivity or as air bubbles and layered solid. The latter structure corresponds to high density. To represent this complicated structure at different porosities, we determine the upper limit to the thermal conductivity for cylinders of the solid and air bubbles and the lower limit for spheres of the solid phase and layers. We then construct a general expression for the thermal conductivity by combining expressions for the upper limit

$$k_u = (1-\varepsilon)k_b + \varepsilon k_c \tag{2}$$

and the lower limit

$$k_l = (1-\varepsilon)k_\ell + \varepsilon k_s. \tag{3}$$

The general expression for the conductivity is written as

$$K = \frac{1}{4}[(3B-1)k_l + (3\Theta-1)k_u + \{[(3B-1)k_c + (3\Theta-1)k_u]^2 + 8k_lk_u\}^{1/2}], \tag{4}$$

where B is the proportion of the deposit consisting of sphere and layers of solid, and $\Theta = 1 - B$.

Measurements on water-vapor frost have been used [2] to derive a formula for B that incorporates the variation in structure over time:

$$B = 13{,}6(B_2-B_1)(\varepsilon-B_1)^2\left[1-\frac{2}{3}\left(\frac{\varepsilon-B_1}{B_3-B_1}+\frac{\varepsilon-B_1}{B_2-B_1}\right)+\frac{(\varepsilon-B_1)^2}{2(B_3-B_1)(B_2-B_1)}\right]. \tag{5}$$

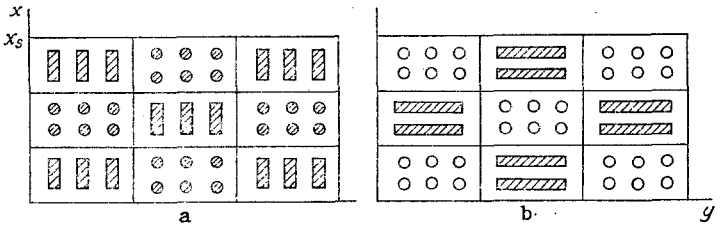

Fig. 1. Models for high-porosity (a) and low-porosity (b) deposit structures.

TABLE 1. Thermophysical Parameters of the Monolithic Solids

Substance	K, W/m·deg	r_c, J/kg	ρ_s, kg/m^3
Freon 13	6,05	$272{,}36\cdot10^3$	1880
Acetone	1,72	$776{,}14\cdot10^3$	848

TABLE 2. Thermal Conductivities of Cryodeposits

Freon 13	ε	0,9	0,8	0,6	0,5	0,4	0,3
	ρ_f, kg/m3	188	377	750	940	1130	1316
	K, W/m × deg	$1{,}86\times10^{-2}$	$2{,}075\times10^{-2}$	$3{,}854\times10^{-2}$	$8{,}857\times10^{-2}$	0,51	1,77

Acetone	ε	0,9	0,7	0,5	0,3
	ρ_f, kg/m3	84,8	254,4	424	593,6
	K, W/m × deg	$4{,}287\times10^{-2}$	$6{,}3\times10^{-2}$	$1{,}162\times10^{-1}$	$7{,}017\times10^{-1}$

The calculations were based on the measured thermophysical properties of monolithic freon 13 and acetone (Table 1), as well as the measured cold-surface temperature T_w, the surface temperature of the deposit T_s, and the partial pressure of the vapor P_v at various points together with the corresponding heat fluxes. In the experiments, the parameters varied over the following ranges: for freon

$$T_w = 77 - 84{,}6,\ T_s = 82{,}4 - 103{,}2\,\text{K};\ P_v/P = 0{,}376 - 0{,}83;$$

and for acetone

$$T_w = 124 - 138{,}4,\ T_s = 157{,}2 - 173{,}5\,\text{K},$$

$$P_v/P = 0{,}125 - 0{,}92.$$

Table 2 gives the calculations.

Least-squares fitting gave the correlations; for freon

$$K = -3.438\cdot10^{-5} + 2{,}145\cdot10^{-7}\rho_f + 1{,}11\cdot10^{-7}\rho_f^2 + 7{,}755\cdot10^{-14}\rho_f^3,$$

and for acetone

$$K = -4{,}855\cdot10^{-3} + 1{,}163\cdot10^{-3}\rho_f - 6{,}455\cdot10^{-6}\rho_f^2 + 1{,}137\cdot10^{-8}\rho_f^3.$$

The consumption of working agent in time is M = Vρt, while the volume of the solid was deduced from geometrical considerations, which gaves an estimate of the density. The calculations and measurements are shown in Fig. 2.

The above method gives good results over a wide range in porosity and can be recommended for determining the thermal conductivity for various deposits. It is possible that one could refine the expression for $B=\sum_{i=0}^{n} a_i\varepsilon^i$, where the a_i are constants or functions of temperature derived from fairly extensive experimental evidence.

The calculations are presented in dimensionless form in Fig. 3 and show that one cannot construct a single curve for all the different materials. One therefore has to determine the individual characteristics.

The solid-state condensation was examined over the pressure range 0.1-1.5 mm Hg. Formulas for free-molecular flow are not applicable in that range, although they are commonly employed in calculations on cryogenic pumps, so we use relationships for continuous media. In particular, we incorporate the effects of diffusion, which plays a basic part in the

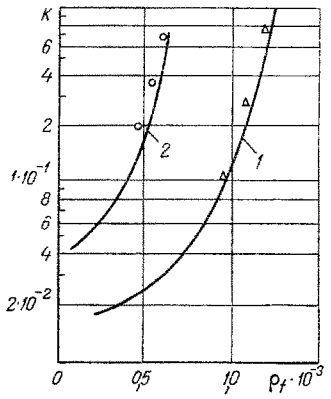

Fig. 2

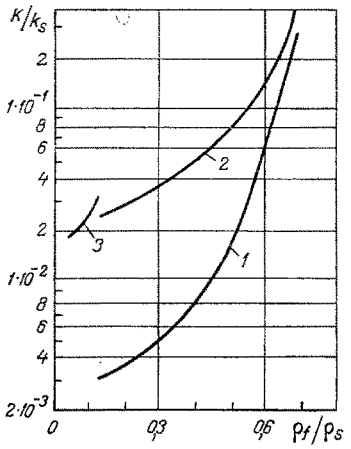

Fig. 3

Fig. 2. Density dependence of the thermal conductivity: 1) freon 13; 2) acetone.

Fig. 3. Variations in thermal conductivity for deposits of various substances: 1) freon 13; 2) acetone; 3) water.

density change. The radiative component of the heat transfer was minimized by an auxiliary screen. To simplify the description, we assumed that the density was constant over the thickness and only varied in time, while the conditions for thermodynamic equilibrium were obeyed within the layer and Clapeyron's equation applied.

The growth can be desribed by an expression of the type $\delta = C[t(T_s - T_w)]^{1/2}$; a theoretical expression has been derived [3] for the thickness on the basis of the theory of crystal growth from the vapor:

$$\delta = 0{,}465\left[\frac{k_s}{r_c\rho_s}t(T_s - T_w)\right]^{1/2}\left[\frac{t}{3600}\right]^{-0{,}03}[T_s - T_w]^{-0{,}01}\Pi^{0{,}25}F, \tag{6}$$

where $\Pi = (P_V - P_F)/(P_{VS} - P_F)$; $F = 1 + 0.052(T_S - T_m)/(T_m - T_w)$.

The energy-balance equation $K(d^2T/dx^2) = -r_c dm/dx$ gives us on the basis of the above assumptions that

$$\frac{d^2T}{dx^2} = -\frac{m_s r_c}{K\delta}. \tag{7}$$

We integrate the equation twice and use the boundary conditions

$$x = 0;\ T = T_w;\ \frac{dT}{dx} = \frac{h(T_a - T_s) + h_m(\rho_{va} - \rho_{vs})r_c}{k_m}, \tag{8}$$

to get the solution as

$$T = -\frac{m_s r_c}{K\delta}\frac{x^2}{2} + \frac{h(T_a - T_s) + h_m(\rho_{va} - \rho_{vs})r_c}{k_m}x + T_w. \tag{9}$$

We substitute $x = \delta$ to get

$$T_s = -\frac{r_c\delta}{2K}\left[\frac{M^2D(1 - \rho_f/\rho_s)r_cP_F}{R^2T_s^3\tau}\frac{h(T_a - T_s) + h_m(\rho_{va} - \rho_{vs})r_c}{k_m\left[1 + \frac{r_c}{K}\frac{M^2D(1 - \rho_f/\rho_s)r_cP_F}{R^2T_s^3\tau}\right]}\right] +$$

$$+ \frac{h(T_a - T_s) + h_m(\rho_{va} - \rho_{vs})r_c}{k_m}\delta + T_w. \tag{10}$$

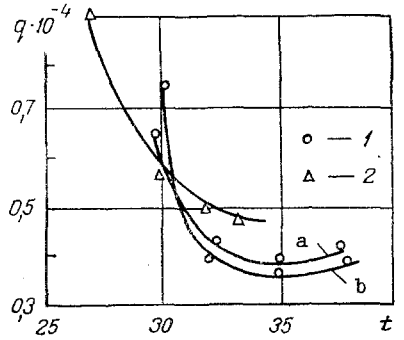

Fig. 4. Heat-flux variation on solid-state condensation under various conditions: 1) freon 13: a) 1.15 mm Hg, 79.2 K; b) 0.536 mm Hg, 79 K; 2) acetone: 0.616 mm Hg, 138 K.

This is a nonlinear equation with parameters dependent on T_s. We determine the heat- and mass-transfer coefficients (h and h_m) via the method proposed in [4]. On solving the integral equations for the boundary layer, we have

$$\mathrm{Nu} = \frac{4}{3}\,0{,}508\psi\,(\mathrm{GrPr})^{1/4}, \tag{11}$$

$$\mathrm{Sh} = \frac{h_m L}{D} = \frac{4}{3}\,\frac{0{,}508\,(\mathrm{Pr})^{1/4}\,(\mathrm{GrPr})^{1/4}}{(1-w_\infty)\,\xi\,(B_3)^{1/4}\,[\mathrm{Pr}+0{,}95B_3]^{1/4}}, \tag{12}$$

where

$$\psi = \frac{\mathrm{Pr}^{1/4}}{B_3^{1/4}\,[\mathrm{Pr}+0{,}95B_3]^{1/4}}; \quad \xi = \left[\frac{(\mathrm{Pr/Sc})(1-w_\infty)}{(1-w_\infty)+(\mathrm{Pr/Sc})^{1/2}(w_\infty - w_w)}\right]^{1/2};$$

$$B_3 = 1 + \mathrm{Pr/Sc}\left[\frac{w_\infty - w_w}{\xi}\right]\left[\frac{1}{1-w_w}\right];$$

in which w is the dimensionless mass fraction of the condensing vapor in the volume and near the surface of the cryodeposit.

The vapor densities are correspondingly $\rho_{va} = P_v M/RT_a$; $\rho_{vs} = P_F M/RT_s$; we derive the vapor pressure by extrapolating the saturation curve $P = \exp(A - B/T)$; the density is found from

$$\frac{d\rho_f}{dt} = \frac{M^2 D\,(1-\rho_f/\rho_s)\,r_c P_F}{R^2 T_s^3\,\tau\delta}\left(\frac{dT}{dx}\right)_s, \tag{13}$$

which is solved numerically together with (10) by the Runge–Kutta method.

The approximate solution to (13) is

$$\rho_f/\rho_s = 1 - \exp\left(-\frac{A}{\rho_s}t\right); \quad A = \frac{M^2 D r_c P_F}{R^2 T_s^3\,\tau\delta}\left(\frac{dT}{dx}\right)_s. \tag{14}$$

The heat flux was calculated from the energy equation, while it was measured from the coolant consumption as $q = Gr_e$.

Comparison of theory and experiment shows that the heat flux at first decreases, but then stabilizes and slowly increases, which is due to increase in the thermal conductivity and heat-transfer surface. Figure 4 shows the variation in heat flux on condensation.

The main effects come from the partial pressure and the cold-surface temperature.

The model based on the diffusion equation is very valuable. It gives good results, although the values are somewhat less than the measured ones, when the surface temperature of the deposit is below the melting point, which was so in our experiments.

NOTATION

K, k_m, effective thermal conductivity of cryodeposit and cold wall, respectively; ρ_f, ρ_s, density of cryodeposit and monolithic solid phase, respectively; r_c, sublimation heat; h, heat-transfer coefficient; h_m, mass-transfer coefficient; δ, thickness of cryodeposit; D, diffusion coefficient; ρ_{va}, ρ_{vs}, vapor density in volume and at surface temperature; T_a, T_w, T_s, T_m, temperature in volume, of the cold wall, of surface, and melting, respectively; P, P_v, P_F, total pressure, partial vapor pressure in volume, and saturation pressure at the surface temperature; k_s, thermal conductivity of the monolithic solid phase; τ, crookedness, $\tau = 1.1$; ε, porosity; B_1, B_2, B_3, parameters in formula (5).

LITERATURE CITED

1. G. Biguria and L. A. Wenzel, "Measurement and correlation of water frost thermal conductivity and density," I.E.C. Fundamentals, 9, No. 1, 129-138 (1970).
2. M. A. Dietenberger, "Generalized correlation of the water frost thermal conductivity," Int. J. Heat Mass Transfer, 26, No. 4, 607-619 (1983).
3. H. W. Schneider, "Frost growth rate equation, forming on cold surfaces," Int. J. Heat Mass Transfer, 21, No. 8, 1019-1024 (1978).
4. R. F. Barron and L. S. Han, "Heat and mass transfer to a cryogenic surface under free-convection conditions," Teploenergetika, No. 4, 84-92 (1965).

ICING ON THE WALLS OF A BURIED PIPELINE BEARING A FREEZING NON-NEWTONIAN LIQUID

V. M. Ovsyannikov

UDC 536.421

The definitive parameters have been derived. Approximate formulas have been obtained for the maximum ice thickness, the time to attain the maximum, and the melting time.

In recent years, a technology has been developed in this country and elsewhere for transporting finely divided highly concentrated suspensions of coal in water [1, 2]. The mixtures travel in pipes in laminar mode or in some cases turbulent. They may have non-Newtonian or pseudoplastic rheological features.

In the design of hydrotransport systems for the harsh climate of Siberia, there is the novel problem of hydrotransport for freezing liquids. The startup period in the winter is particularly hazardous from the viewpoint of freezing, when the soil around the pipeline has not yet been heated and has a temperature below the freezing point of the liquid.

The fullest analysis of the icing problem in the Russian literature is to be found in [3]. In [4], icing calculations were compared with measurements for laminar flow of a Newtonian liquid, and a confirmation of the model formulation was obtained. In [3, 4], there are mainly calculations on the steady-state icing. Ice growth and thawing have been examined in [5, 6]. We now present the formulation.

The pipeline is buried in ground whose temperature at the start is below the freezing point of the liquid. A layer of frozen suspension is formed on the inside, which for brevity

---

All-Union Research and Development Institute for the Pipeline Hydrotransport Industry.

Translated from Inzhenerno-Fizicheskii Zhurnal, Vol. 50, No. 2, pp. 285-293, February, 1986. Original article submitted November 27, 1984.

0022-0841/86/5002-0212$12.50